Intense Visible and Near-Infrared Upconversion Photoluminescence in Colloidal LiYF₄:Er³⁺ Nanocrystals under Excitation at 1490 nm

Guanying Chen[†,‡], **Tymish Y. Ohulchanskyy**[†], **Aliaksandr Kachynski**[†], **Hans Ågren**[‡], and **Paras N. Prasad**[†,*]

[†]Institute for Lasers, Photonics, and Biophotonics, The State University of New York at Buffalo, Buffalo, New York 14260

[‡]Department of Theoretical Chemistry, Royal Institute of Technology, S-10691 Stockholm, Sweden

Abstract

We report intense upconversion photoluminescence (PL) in colloidal LiYF₄:Er³⁺ nanocrystals under excitation with telecom-wavelength at 1490 nm. The intensities of two- and three-photon anti-Stokes upconversion PL bands are higher than or comparable to that of the Stokes emission under excitation with low power density in the range of 5–120 W/cm². The quantum yield of the upconversion PL was measured to be as high as ~1.2±0.1%, which is almost 4 times higher than the highest upconversion PL quantum yield reported up to date for lanthanide-doped nanocrystals in 100 nm sized hexagonal NaYF₄:Yb³⁺20%, Er³⁺2% using excitation at ~980 nm. Power dependence study revealed that the intensities of all PL bands have linear dependence on the excitation power density, which was explained by saturation effects in the intermediate energy states.

Keywords

near-infrared; upconversion photoluminescence; nanocrystals; lanthanide; telecommunications

Lanthanide-doped nanocrystals can convert the absorbed light with lower energy, usually in the near infrared (NIR) range, into the photoluminescence (PL) emission with higher energy in the ultraviolet, visible, or NIR ranges.[1–3] Because of the existence of real intermediate energy levels in lanthanide ions,[2] this upconversion process is much more efficient than the conventional multiphoton absorption induced fluorescence where the intermediate levels are virtual.[4] An efficient energy upconversion in nanocrystals is highly desirable for numerous applications, such as displays,[5,6] PL imaging,[7–14] photodynamic therapy,[15–19] *etc.* Lanthanide-doped upconversion nanocrystals are also excellent candidates for improving solar cell efficiency by harvesting energy in the NIR range due to their ladder-like system of energy levels.[20–22]

*Corresponding Author. pnprasad@buffalo.edu.

Despite recent progresses in the synthesis and design of lanthanide-doped nanocrystals,[23–27] it is still of great challenge to obtain an efficient upconversion PL since the intensity of anti-Stokes upconversion PL is usually much lower than that of the Stokes emission.[3] Furthermore, upconversion PL generally show a higher power dependence on the excitation intensity, thus requiring an intense source to generate it. Fluoride nanocrystals are known to possess host lattice of low phonon energy, which results in decreased nonradiative relaxations and, in turn, in relatively high upconversion PL efficiency.[28–30] Although optical properties of trivalent lanthanide ions have been widely studied in several fluoride matrices in the bulk, investigations on their corresponding dispersible nanocrystals are mostly restricted to $NaYF_4$.[31–35] Nanocrystals of $NaYF_4$ (10–100 nm sized) codoped with Yb^{3+} and Er^{3+} ions, are now considered to be among the most efficient upconversion nanocrystals, exhibiting visible emission under excitation at ~ 980 nm, with the upconversion PL quantum yield of ~0.005–0.3%.[36–38] An efficient conversion of telecomm-wavelength (1.3–1.55 μm) into visible or NIR light is of particular importance due to their potential uses in frequency upconversion lasing,[39,40] photovoltaics,[20,41] IR quantum counter,[1] detection of surface plasmons,[42] displays and sensors.[43] The Er^{3+} ions are well suitable for these endeavors owing to their absorption at ~1500 nm, which corresponds to the $^4I_{13/2}$ energy level.[1] However, a lack of efficient sensitizers (like Yb^{3+} ions at ~980 nm) and a suitable host matrix for upconversion of ~1.5 μm has limited the study of this technologically important process.

The $LiYF_4$ can be considered as a suitable fluoride host lattice for the upconversion processes under excitation at ~1.5 μm, since Er^{3+} ions have long-lived intermediate states in this low-phonon lattice (*e.g.*, $^4I_{13/2}$ with a characteristic lifetime of ~10 ms).[44–46] These intermediate excited energy states with long lifetime can act as energy reservoirs when populating higher energy levels. In this case, upconversion might work by a more effective one-photon mechanism, leading to efficient upconversion PL generation under lower power excitation.[47–49] Despite these unique features, investigations of the upconversion PL in Er^{3+}-doped $LiYF_4$ under excitation at ~1.5 μm are surprisingly limited. Most of the studies on Er^{3+}-doped $LiYF_4$ are devoted to laser output at ~2.7–3.0 μm or green/red upconversion under excitation at 980 nm.[44–46] Using $LiYF_4$ single crystal doped with Er^{3+}, the upconversion laser action at cryogenic temperatures in the visible range (~0.55 μm) under excitation at ~1.5 μm was reported two decades ago,[50,51] but was not noticeably utilized since then. On the other hand, investigations of lanthanide-doped colloidal nanocrystals of $LiYF_4$ are extremely limited and only involve upconversion of ~980 nm excitation to the visible range.[52–55]

In this work, we report intense upconversion PL in colloidal $LiYF_4$:Er^{3+} nanocrystals using excitation at the telecom-wavelength of 1490 nm. Under excitation with low power density, the intensities of the anti-Stokes PL emission bands (three-photon induced PL bands peaked at 550 and 670 nm and two-photon induced emission with maximum at ~970 nm) are comparable to and higher than the one-photon induced Stokes emission at ~1.5 μm.

RESULTS AND DISCUSSIONS

Nanocrystals of $LiYF_4$:Er^{3+} Displaying Intense Visible and NIR Upconversion Photoluminescence

The colloidal $LiYF_4$:Er^{3+} nanocrystals were synthesized *via* modification from a thermolysis procedure.[7] As one can see in Figure 1A, the resulting nanocrystals are of spindle shape and monodisperse. They have a uniform aspect ratio (length/breadth) of about 1.9; the average length was evaluated to be about 85 nm. A high-resolution TEM (HRTEM) image (Supporting Information, Figure S1) distinguishes the lattice arrangement of the atoms in one individual nanoparticle, indicating high crystallinity of the prepared nanoparticles. A

selected area electron diffraction pattern in Figure 1B demonstrates the formation of tetragonal phase of the nanocrystals and is indexed to the corresponding (hkl) planes of the standard JCPDS 85-0806 $LiYF_4$ structure. The prepared $LiYF_4:Er^{3+}$ nanocrystals form transparent and stable colloidal suspension in chloroform (Figure 1C). These colloidal nanocrystals produce upconversion PL under excitation at 1490 nm with unfocused laser beam of 4 W/cm^2, which appears bright green to the naked eye, as one can see in Figure 1D (See also Supporting Information, Figure S2).

The PL spectrum of colloidal $LiYF_4$ nanocrystals doped with 10% Er^{3+} ions under laser excitation at 1490 nm are shown in Figure 2. The shape of PL spectra remains almost the same in a wide range of excitation power density due to a close to linear dependence of all PL bands (Figure 3). Four upconversion PL bands are clearly resolved; they have maxima at 550, 670, 800, and 970 nm, which correspond to transitions from the $^2H_{11/2}/^4S_{3/2}$, $^4F_{9/2}$, $^4I_{9/2}$, and $^4I_{11/2}$ to the ground $^4I_{15/2}$ state of Er^{3+}, respectively.[20] The long wavelength edge of ~800 nm band might also be contributed by the $^4S_{3/2} \rightarrow ^4I_{13/2}$ transition (Figure 4). In addition to the upconversion PL, the Stokes radiation at 1500 nm was also displayed which corresponds to the transition $^4I_{13/2} \rightarrow ^4I_{15/2}$ of the Er^{3+} ions. The intensities of the anti-Stokes emission generated by multiphoton processes are usually tens times lower than those of Stokes emission for low power density excitation, due to their inefficient generation mechanism. For example, three-photon blue emissions at 480 nm in hexagonal bulk $NaYF_4$: 0.3% Tm^{3+}, 25% Yb^{3+} crystals (the most efficient blue emitter) is about 46 times less than the Stokes emission under 980 nm excitation of 80 W/cm^2.[38] It is striking that the anti-Stokes, two-photon induced emission at ~975 nm is more intense than the Stokes emission at 1500 nm, while the three-photon induced upconversion PL at 550 and 670 nm are comparable to that, suggesting an extremely efficient upconversion mechanism here. An upconversion quantum yield (UCQY) were measured to be about 0.13±0.02% and 0.07±0.02% for three-photon green and red upconversion PL, while for the two-photon NIR emission at 800 and 970 nm they were evaluated to be about 0.05±0.01% and 0.95±0.05% under 1490 nm excitation of 150 W/cm^2 (Supporting Information, Part II). The total quantum yield for the visible and the NIR emission is 1.2±0.1%, which is almost 4 times higher than the highest UCQY reported in the literature for the upconversion nanocrystals (100 nm sized hexagonal $NaYF_4$:20%Yb^{3+}/2%Er^{3+} nanocrystals under 980 nm excitation with 150 W/cm^2).[36]

The effect of the Er^{3+} ion concentration on the upconversion emission bands was also investigated (Figure 2, inset). As one can see, the intensity of upconversion PL increases slightly with the increase in the content of Er^{3+} ions from 5% to 20%, and remains nearly unchanged for Er^{3+} concentrations of 20% and 30% ions, due to the concentration quenching effect.[1] The PL spectra normalized to the Er^{3+} content show that the nanocrystal $LiYF_4:Er^{3+}$ with 10% Er^{3+} has the highest upconversion efficiency (Supporting Information, Figure S6). It should be noted that the ratio of the intensities of the green band at ~550 nm and the red one at ~670 nm (green-to-red ratio, GRR) is tuned by the Er^{3+} ion concentration; an increase in the content of Er^{3+} ions induces a decrease in GRR. This feature enables us to manipulate the color output of the colloidal nanocrystals $LiYF_4:Er^{3+}$ by adjusting the Er^{3+} ion concentration.

Pump Power Dependence and Mechanisms of Intense Visible and NIR Upconversion Photoluminescence

Figure 3 shows the measured pump power dependences of all PL bands for the colloidal $LiYF_4$ nanocrystals doped with 10% of Er^{3+} ions. The number of photons required to populate the upper emitting state can be obtained from the equation $I_{PL} \propto P^n$, where I_{PL} is the PL intensity, P is the pump laser power, and n is the number of the laser photons.[47–49] It is known that when upconversion PL is excited by sequential absorption and energy transfer

upconversion of n photons, its dependence on the absorbed pump power P decreases from P^n down to P^1 as long as the upconversion rate well exceeds the decay rate for the intermediate states. This applies for the highest energy electronic state that is excited through upconversion, while lower-lying states (excited by upconversion with m photons, where m<n) were predicted to have a power dependence even less than P^1.[48,49]

As shown in Figure 3, the dependence of intensity of the upconversion PL bands on the laser power for low excitation power density range of 5–120 W/cm^2 is overall close to linear, with lesser slope for PL arising from lower energy states. This result explains the high intensity of anti-Stokes emission versus the Stokes one (Figure 2), since an inefficient multiphoton upconversion mechanism has been switched to an efficient one-photon-like mechanism. The power dependences of the PL emission were also measured for excitation power density lower than 5 W/cm^2 (range of ~0.3–4.5 W/cm^2; Supporting Information, Figure S7). It was found that although the slope value for power dependence of Stokes emission at 1500 nm remains the same as in Figure 3, those for three-photon (peaks at 550 and 669 nm) and two-photon (850 and 1000 nm) emissions increase as compared to the corresponding power dependencies shown in Figure 3. It should be noted that a power density as high as 150 W/cm^2 had to be used in 100 nm sized hexagonal NaYF$_4$:20% Yb^{3+}/ 2%Er^{3+} nanocrystals to achieve the onset saturation under 980 nm excitation.[36] In our case, saturation occurs at much lower power density, which also illustrates the high efficiency of upconversion in the colloidal LiYF$_4$:Er^{3+} nanocrystals under 1490 nm excitation. It is worth noting that the upconversion emission of the sample under study was visible to the naked eye at the excitation power as low as ~0.3 W/cm^2. To further clarify the upconversion mechanism, we have measured the PL decays at 1535, 1005, 548, and 667 nm (which correspond to the $^4I_{13/2}$, $^4I_{11/2}$, $^4S_{3/2}$, and $^4F_{9/2}$ states of Er^{3+} ions) (Supporting information, Figures S8–S11). The average lifetimes of $^4I_{13/2}$ and $^4I_{11/2}$ states were evaluated to be about 5.4–10 ms and 1.5–2.4 ms in colloidal LiYF$_4$:Er^{3+} nanocrystals, respectively; while lifetimes of ~56–136 µs and ~63–120 µs were measured for emission from the $^4S_{3/2}$, and $^4F_{9/2}$ states under direct excitation using 532 nm. These short lifetimes of emission from the upper states under direct excitation, along with long lifetimes of the intermediate states, suggest that the long-lived intermediate energy states are important to realize high efficiency of upconversion owing to their strong reservoir capability and low energy losses.[47]

Figure 4 shows the energy levels of Er^{3+} ions as well as the proposed upconversion pathways under laser excitation with 1490 nm.[56] First, laser photons directly excite the Er^{3+} ions from the ground $^4I_{15/2}$ state to the long-lived $^4I_{13/2}$ state which results in Stokes emission at ~1500 nm. Different processes can then lead to the population of higher excited Er^{3+} states, which rely either on multistep excited state absorption or energy transfer upconversion mechanisms. Since the concentration of Er^{3+} ions in all synthesized LiYF$_4$ nanocrystals is high enough, it is plausible that energy transfer upconversion is the dominant mechanism due to the strong multipolar ion-ion interactions induced by the short ion-ion distance.[1] With the assistance of lattice phonons, the Er^{3+} ion at the $^4I_{13/2}$ state can be consecutively promoted to the $^4I_{9/2}$ and the $^2H_{11/2}$/$^4S_{3/2}$ states *via* energy transfers from Er^{3+} ions at the excited $^4I_{13/2}$ state. Radiative decay from the $^2H_{11/2}$/$^4S_{3/2}$ state to the ground state generates an intense three-photon green emission with maxima at ~520/550 nm. Subsequently, nonradiative relaxations from this state populate the $^4F_{9/2}$ state, from which strong three-photon red emissions with peak at ~670 nm are produced. Similarly, the radiative decay from the $^4I_{9/2}$ to the ground state generates a weak two-photon emission at ~800 nm, while nonradiative relaxation from this state populates the $^4I_{11/2}$ state, from which a two-photon radiation with maximum at 970 nm is emitted. We would like to emphasize that the radiative decay from $^4I_{11/2}$ to $^4I_{13/2}$ can generate emission at ~2.7–3 µm, which is known to be utilized for laser output in bulk crystals of LiYF$_4$:Er^{3+}.[44–46] The 2.7–3 µm range is beyond the detection range of our spectroscopy setup, but we assume that the

intensity of the $^4I_{11/2} \rightarrow {}^4I_{13/2}$ PL in LiYF$_4$:Er^{3+} nanocrystals can be estimated from the branch ratio of the $^4I_{11/2} \rightarrow {}^4I_{13/2}$ transition in the LiYF$_4$ crystal, which was found to be about 2/3 times the intensity of the 970 nm peaked emission ($^4I_{11/2} \rightarrow {}^4I_{15/2}$ transition).[45] The cross relaxation process $^2H_{11/2}/^4S_{3/2} + {}^4I_{11/2} \rightarrow 2^4F_{9/2}$ (Figure 4) might play an important role in tuning the GRR.[57] An increase in the Er^{3+} ion concentration enforces the Er^{3+}-Er^{3+} interaction due to the shorter ion-ion distance, and, thus, leads to higher cross relaxation rates. The increased cross relaxation rates will cause a decrease in the GRR with the increase of Er^{3+} ions, which is in good agreement with the observation shown in the inset of Figure 2. It should be noted that since the lifetime in the intermediate states of Er^{3+} ions is long enough (See Supporting information, Figures S8 and S9), upconversion rates in these states might be able to readily exceed their radiative decay rates and induce serious saturation effects even under low energy light excitation.[47] This important feature causes a change of the multi-photon mechanism of population of the upper energy states into one-photon-like mechanism, thereby leading to intense upconversion PL in colloidal LiYF$_4$:Er^{3+} nanocrystals (Figures 2 and 3).

CONCLUSIONS

To summarize, we demonstrate highly efficient upconversion PL in colloidal LiYF$_4$:Er^{3+} nanocrystals under excitation with telecom-wavelength at 1490 nm. The intensities of two- (970 nm peak) and three-photon (maxima at ~550 and ~670 nm) anti-Stokes upconversion PL bands are higher than or comparable to that of the Stokes emission (at ~1500 nm) under low power excitation. The total upconversion PL quantum yield under excitation with 1490 nm was measured to be as high as 1.2±0.1%, which is almost 4 times higher than the UCQY for the most efficient upconversion nanocrystals reported up to date (100 nm sized hexagonal NaYF$_4$:20%Yb^{3+}/2%Er^{3+} nanocrystals under excitation at 980 nm). In addition, the intensities of all PL bands were shown to depend linearly on the excitation power in low power density range (5–120 W/cm^2), which was explained by saturation effects in the intermediate energy states. This work might evoke wide interests in biophotonic and photonic applications of these nanocrystals.

METHODS

Synthesis of Er^{3+} Doped Nanocrystals LiYF$_4$

Nanocrystals of LiYF$_4$ doped with 5, 10, 15, 20, and 30% of Er^{3+} ions were synthesized by thermal decomposition of lanthanide and lithium trifluoroacetate precursors in the presence of oleic acid coordinating ligands and noncoordinating 1-octadecene solvent molecules. All chemicals used in the synthesis were purchased from Sigma-Aldrich and used as received. In the case of LiYF$_4$:Er^{3+} 10% nanocrystals, 0.166g (2.25 mmol) Li$_2$CO$_3$, 0.048 g Er$_2$O$_3$ (0.125 mmol), 0.254 g Y$_2$O$_3$ (1.125 mmol) were dissolved in 50% concentrated trifluoroacetic acid at 95 °C in a three-necked 100 mL flask. Then, the solutions were evaporated to dryness under the argon gas purge. Next, 30 mL oleic acid (90%, technical grade) and 30 mL 1-octadecene (90%, technical grade) were added into the three-necked flask. The resulting solution was then heated at 120°C with magnetic stirring for 30 minutes to remove water and oxygen. The brown solution was then heated to 330 °C at a rate of about 8 °C per min under argon gas protection, and kept at this temperature under vigorous stirring for about 1 h. A syringe needle was used to let the argon gas out during the synthesis. The mixture was cooled to room temperature and precipitated by acetone in an ultrasonic bath and collected by centrifugation at 11000 rpm for 10 min. The precipitate was washed with ethanol for several times, and the nanocrystals were dispersed in 10 mL of chloroform for further characterizations.

Instruments

The size and morphology of the nanocrystals were characterized by TEM microscopy using a JEM-2010 microscope at an acceleration voltage of 200 KV. Upconversion PL spectra in the range of 480–1300 nm were recorded using an EPP 2000 fiber spectrofluorometer (Stellar Net Inc.). Synchronously, a SPEX 270M spectrometer (Jobin Yvon), equipped with an InGaAs TE-cooled photodiode (Electro- Optical Systems, Inc.), was used to record PL spectra in the range of 900–1700 nm. The two PL spectra were matched at the overlapped 970 nm emissions to present the whole spectra of 480–1700 nm. All PL spectra have been corrected for the spectral sensitivity of the spectral systems using as a reference the black body emission of a tungsten bulb with color temperature of about 2900 K.[58] Laser excitation of 971 nm or 1490 nm was provided by a tunable optical parametric oscillator (OPO, Levante Emerald, APE, Germany) pumped by the second harmonic of Nd:YVO$_4$ laser (High Q Laser, Australia) emitting at 532 nm with a pulse width of 6 ps and a repetition rate of 76 MHz. The emission signal of the sample in the cuvette was collected at 90° relative to the excitation light. Absorption spectra of nanocrystals colloidal suspension were acquired using a Shimadzu 3600 UV–Visible-NIR spectrophotometer. The PL decay profiles at 1500 nm and 1005 nm were recorded at the Infinium oscilloscope (Hewlett-Packard) coupled to a thermoelectric cooled NIR photomultiplier tube (Hamamatsu, H10330-45 NIR-PMT) which was attached to the second output of the SPEX 270M spectrometer. The laser diode from QPhotonics operating at 975 nm was used in a pulsed mode as an excitation source. The decays of the emissions at 548 nm and at 667 nm were recorded at the Infinium oscilloscope (Hewlett-Packard) coupled to the PMT of Fluorolog-3.11 Jobin Yvon spectrofluorometer. A second harmonic (532 nm) from a nanosecond pulsed Nd:YAG laser (Lotis TII, Belarus) operating at 20 Hz was used as the excitation source in this case. Photographic images of UC nanocrystals colloidal were taken by a digital camera (Lumix DMC-Fx520, Japan) without any filter or image processing.

Supplementary Material

Refer to Web version on PubMed Central for supplementary material.

Acknowledgments

REFERENCES AND NOTES

1. Auzel F. Upconversion and Anti-Stokes Processes with f and d Ions in Solids. Chem Rev. 2004; 104:139–173. [PubMed: 14719973]

2. Wang F, Liu X. Recent Advances in the Chemistry of Lanthanide-Doped Upconversion Nanocrystals. Chem Soc Rev. 2009; 38:976–989. [PubMed: 19421576]

3. Suyver J, Aebischer A, Biner D, Gerner P, Grimm J, Heer S, Krämer K, Reinhard C, Güdel H. Novel Materials Doped with Trivalent Lanthanides and Transition Metal Ions Showing Near-Infrared to Visible Photon Upconversion. Opt Mater. 2005; 27:1111–1130.

4. He GS, Tan LS, Zheng Q, Prasad PN. Multiphoton Absorbing Materials: Molecular Designs, Characterizations, and Applications. Chem Rev. 2008; 108:1245–1330. [PubMed: 18361528]

5. Sivakumar S, Veggel F, Raudsepp M. Bright White Light through Upconversion of a Single NIR Source from Sol-Gel-Derived Thin Film Made with Ln-Doped LaF$_3$ Nanoparticles. J Am Chem Soc. 2006; 127:12464–12465. [PubMed: 16144374]

6. Cai R, Lian H, Hou Z, Zhang C, Peng C, Lin J. Preparation and Characterization of Upconversion Luminescent NaYF$_4$:Yb^{3+}, Er^{3+}(Tm^{3+}) PMMA Bulk Transparent Nanocomposites Through In Situ Photopolymerization. J Phys Chem C. 2010; 114:610–616.

7. Nyk M, Kumar R, Ohulchanskyy T, Bergey E, Prasad PN. High Contrast *in Vitro* and *in Vivo* Photoluminescence Bioimaging Using Near Infrared to Near Infrared Upconversion in Tm^{3+} and Yb^{3+} Doped Fluoride Nanophosphors. Nano Lett. 2008; 8:3834–3838. [PubMed: 18928324]

8. Wu S, Han G, Milliron D, Aloni S, Altoe V, Talapin D, Cohen B, Schuck P. Non-blinking and Photostable Upconverted Luminescence from Single Lanthanide-Doped Nanocrystals. Proc Natl Acad Sci U S A. 2009; 106:10917–10921. [PubMed: 19541601]

9. Chatterjee D, Rufaihah A, Zhang Y. Upconversion Fluorescence Imaging of Cells and Small Animals Using Lanthanide Doped Nanocrystals. Biomaterials. 2008; 29:937–943. [PubMed: 18061257]

10. Zhou J, Sun Y, Du XX, Xiong LQ, Hu H, Li FY. Dual-Modality *in Vivo* Imaging Using Rare-Earth Nanocrystals with Near-Infrared to Near-Infrared (NIR-to-NIR) Upconversion Luminescence and Magnetic Resonance Properties. Biomaterials. 2010; 31:3287–3295. [PubMed: 20132982]

11. Liu Q, Sun Y, Li CG, Zhou J, Li CY, Yang TS, Zhang XZ, Yi T, Wu DM, Li FY. ^{18}F-Labeled Magnetic-Upconversion Nanophosphors *via* Rare-Earth Cation-Assisted Ligand Assembly. ACS Nano. 2011; 5:3146–3157. [PubMed: 21384900]

12. Zhou J, Yu MX, Sun Y, Zhang XZ, Zhu XJ, Wu ZH, Wu DM, Li FY. Fluorine-18-labeled Gd^{3+}/ Yb^{3+}/Er^{3+}-codoped $NaYF_4$ Nanophosphors for Multimodality PET/MR/UCL Imaging. Biomaterials. 2011; 32:1148–1156. [PubMed: 20965563]

13. Cao TY, Yang Y, Gao Y, Zhou J, Li ZQ, Li FY. High-Quality Water-Soluble and Surface-Functionalized Upconversion Nanocrystals as Luminescent Probes for Bioimaging. Biomaterials. 2011; 32:2959–2968. [PubMed: 21262531]

14. Wang M, Mi CC, Wang WX, Liu CH, Wu YF, Xu ZR, Mao CB, Xu SK. Immunolabeling and NIR-Excited Fluorescent Imaging of HeLa Cells by Using $NaYF_4$:Yb, Er Upconversion Nanoparticles. ACS Nano. 2009; 3:1580–1586. [PubMed: 19476317]

15. Prasad, PN. Introduction to Biophotonics. Wiley-Interscience; New York: 2003. p. 534-535.

16. Zhang P, Steelant W, Kumar M, Scholfield M. Versatile Photodyanmic Therapy at Infrared Excitation. J Am Chem Soc. 2007; 129:4526–4527. [PubMed: 17385866]

17. Qian H, Guo H, Ho P, Mahendran R, Zhang Y. Mesoporous-Silica-Coated Upconversion Fluorescent Nanoparticles for Photodynamic Therapy. Small. 2009; 5:2285–2290. [PubMed: 19598161]

18. Wang F, Banerjee D, Liu YS, Chen XY, Liu XG. Upconversion Nanoparticles in Biological Labeling, Imaging, and Therapy. Analyst. 2010; 135:1839–1854. [PubMed: 20485777]

19. Mader H, Kele P, Saleh S, Wolfbeis O. Upconverting Luminescent Nanoparticles for Use in Bioconjugation and Bioimaging. Curr Opin Chem Biol. 2010; 14:582–596. [PubMed: 20829098]

20. Shalav A, Richards B, Trupke T, Krämer K, Güdel H. Application of $NaYF_4$:Er^{3+} Upconverting Phosphors for Enhanced Near-Infrared Silicon Solar Cell Response. Appl Phys Lett. 2005; 86:013505.

21. Ende B, Aarts L, Meijerink A. Lanthanide Ions as Spectral Converters for Solar Cells. Phys Chem Chem Phys. 2009; 11:11081–11095. [PubMed: 20024374]

22. Richards B. Enhancing the Perfomance of Silicon Solar Cells *via* the Application of Passive Luminescence Conversion Layers. Sol Energy Mater Sol Cells. 2006; 90:2329–2337.

23. Wang F, Han Y, Lim CS, Lu Y, Wang J, Xu J, Chen H, Zhang C, Hong M, Liu X. Simultaneous Phase and Size Control of Upconversion Nanocrystals through Lanthanide Doping. Nature. 2010; 463:1061–1065. [PubMed: 20182508]

24. Ye X, Collins JE, Kang Y, Chen J, Chen D, Yodh A, Murray C. Morphologically Controlled Synthesis of Colloidal Upconversion Nnaophosphors and Their Shape-Directed Self-Assembly. Proc Natl Acad Sci U S A. 2010; 107:22430–22435. [PubMed: 21148771]

25. Chen D, Yu Y, Huang F, Huang P, Yang A, Wang Y. Modifying the Size and Shape of Monodisperse Bifunctional Alkaline-Earth Fluoride Nanocrystals through Lanthanide Doping. J Am Chem Soc. 2010; 132:9976–9978. [PubMed: 20593808]

26. Wang H, Nann T. Monodisperse Upconverting Nanocrystals by Microwave-Assisted Synthesis. ACS Nano. 2009; 3:3804–3808. [PubMed: 19873986]

27. Chen G, Ohulchanskyy T, Kumar R, Ågren H, Prasad PN. Ultrasmall Monodisperse $NaYF_4:Yb^{3+}/Tm^{3+}$ Nanocrystals with Enhanced Near-Infrared to Near-Infrared Upconversion Photoluminescence. ACS Nano. 2010; 4:3163–3168. [PubMed: 20509664]

28. Wang G, Peng Q, Li Y. Upconversion Luminescence of Monodisperse $CaF_2:Yb^{3+}/Er^{3+}$ Nanocrystals. J Am Chem Soc. 2009; 131:14200–14201. [PubMed: 19775118]

29. Wang G, Peng Q, Li Y. Synthesis and Upconversion Luminescence of $BaY_2F_8:Yb^{3+}/Er^{3+}$ Nanobelts. Chem Commun. 2010; 46:7528–7529.

30. Liu Y, Tu D, Zhu H, Li R, Luo W, Chen X. A Strategy to Achieve Efficient Dual-Mode Luminescence of Eu^{3+} in Lanthanide Doped Multifunctional $NaGdF_4$ Nanocrystals. Adv Mater. 2010; 22:3266–3271. [PubMed: 20533416]

31. Mai H, Zhang Y, Si R, Yan Z, Sun L, You L, Yan C. High-Quality Sodium Rare-Earth Fluoride Nanocrystals: Controlled Synthesis and Optical Properties. J Am Chem Soc. 2006; 128:6426–6436. [PubMed: 16683808]

32. Boyer J, Vetrone F, Cuccia L, Capobianco J. Synthesis of Colloidal Upconverting $NaYF_4$ Nanocrystals Doped with Er^{3+}, Yb^{3+} and Tm^{3+}, Yb^{3+} *via* Thermal Decomposition of Lanthanide Trifluoroacetate Precursors. J Am Chem Soc. 2006; 128:7444–7445. [PubMed: 16756290]

33. Heer S, Kömpe K, Güdel H, Haase M. Highly Efficient Multicolour Upconversion Emission in Transparent Colloids of Lanthanide-Doped $NaYF_4$ Nanocrystals. Adv Mater. 2004; 16:2102–2105.

34. Zhang F, Wan Y, Yu T, Zhang F, Shi Y, Xie S, Li Y, Xu L, Tu B, Zhao D. Uniform Nanostructured Arrays of Sodium Rare-Earth Fluorides for Highly Efficient Multicolor Upconversion Luminescence. Angew Chem Int Ed. 2007; 46:7976–7979.

35. Shan J, Ju Y. Controlled Synthesis of Lanthanide-Doped $NaYF_4$ Upconversion Nanocrystals *via* Ligand Induced Crystal Phase Transition and Silica Coating. Appl Phys Lett. 2007; 91:123103.

36. Boyer J, Veggel F. Absolute Quantum Yield Measurements of Colloidal $NaYF_4:Er^{3+}$, Yb^{3+} Upconverting Nanoparticles. Nanoscale. 2010; 2:1417–1419. [PubMed: 20820726]

37. Page R, Schaffers K, Waide P, Tassano J, Payne A, Krupke W. Upconversion-Pumped Luminescence Efficiency of Rare-Earth-Doped Hosts Sensitized with Trivalent Ytterbium. J Opt Soc Am B. 1998; 15:996–1008.

38. Suyver J, Grimm J, Veen M, Biner D, Krämer K, Güdel H. Upconversion Spectroscopy and Properties of $NaYF_4$ Doped with Er^{3+}, Tm^{3+} and/or Yb^{3+} J Lumin. 2006; 117:1–12.

39. He GS, Markowicz P, Lin TC, Prasad PN. Observation of Stimulated Emission by Direct Three-Photon Excitation. Nature. 2002; 415:767–770. [PubMed: 11845202]

40. Zheng K, Zhao D, Zhang D, Liu N, Qin W. Ultraviolet Upconversion Fluorescence of Er^{3+} Induced by 1560 nm Laser Excitation. Opt Lett. 2010; 15:2442–2444. [PubMed: 20634857]

41. Ivanova S, Pellé F. Strong 1.53 µm to NIR-VIS-UV Upconversion in Er-Doped Fluoride Glass for High-Efficiency Solar Cells. J Opt Soc B. 2009; 29:1930–1938.

42. Verhagen E, Kuipers L, Polman A. Enhanced Nonlinear Optical Effects with a Tapered Plasmonic Waveguide. Nano Lett. 2007; 7:334–337. [PubMed: 17297997]

43. Maciel G, Rakov N, Fokine M, Carvalho C, Pinheiro C. Strong Upconversion from $Er_3Al_5O_{12}$ Ceramic Powders Prepared by Low Temperature Direct Combustion Synthesis. Appl Phys Lett. 2006; 89:08119.

44. Jensen T, Diening A, Huber G, Chai B. Investigation of Diode-Pumped 2.8 µm $Er:LiYF_4$ Lasers with Various Doping Levels. Opt Lett. 1996; 21:585–587. [PubMed: 19876091]

45. Pollnau M, Spring M, Ghisler C, Wittwer S, Lüthy W, Weber H. Efficiency of Erbium 3- µm Crystal and Fiber Lasers. IEEE Quantum Electron. 1996; 32:657–663.

46. Wetter N, Deana A, Ranieri I, Gomes L, Baldochi S. Influence of Excited-State-Energy Upconversion on Pulse Shape in Quasi-Continous-Wave Diode-Pumped $Er:LiYF_4$ Lasers. IEEE Quantum Electron. 2010; 46:99–103.

47. Chen G, Liang H, Liu H, Somesfalean G, Zhang Z. Near Vacuum Ultraviolet Luminescence of Gd^{3+} and Er^{3+} Ions Generated by Super Saturation Upconversion Processes. Opt Exp. 2009; 17:16366–16371.

48. Pollnau M, Gamelin D, Lüthi D, Güdel H. Power Dependence of Upconversion Luminescence in Lanthanide and Transition-Metal-Ion Systems. Phys Rev B. 2000; 61:3337–3346.

49. Suyver JF, Aebischer A, García-Revilla S, Gerner P, Güdel HU. Anomalous Power Dependence of Sensitized Upconversion Luminescence. Phys Rev B. 2005; 71:125123.

50. Xie P, Rand S. Visible Cooperative Upconversion Laser in Er:LiYF$_4$. Opt Lett. 1992; 17:1198–1200. [PubMed: 19798132]

51. Xie P, Rand S. Nonlinear Dynamics of Cooperative Upconversion. J Opt Soc Am B. 1994; 11:901–912.

52. Mahalingam V, Vetron F, Naccache R, Speghini A. Capobianco. Colloidal Tm^{3+}/Yb^{3+}-Doped LiYF$_4$ Nanocrystals: Multiple Luminescence Spanning the UV to NIR Regions *via* Low-Energy Excitation. Adv Mater. 2009; 21:4025–4028.

53. Wang J, Wang F, Xun J, Wang Y, Liu Y, Chen X, Chen H, Liu X. Lanthanide-Doped LiYF$_4$ Nanocrystals: Synthesis and Multicolor Upconversion Tuning. CR Chime. 2010; 13:731–736.

54. Du Y, Zhan Y, Sun L, Yan C. Optically Active Uniform Potassium and Lithium Rare-Earth Fluoride Nanocrystals Derived from Metal Trifluoacetate Precursors. Dalton Trans. 2009:8574–8581. [PubMed: 19809734]

55. Yi G, Lee W, Chow G. Synthesis of LiYF$_4$, BaYF$_5$ and NaLaF$_4$ Optical Nanocrystals. J Nanosci Nanotech. 2009; 7:2790–2794.

56. Brown M, Roots K, Shand W. Energy Levels of Er^{3+} in LiYF$_4$. J Phys C. 1969; 2:593–602.

57. Capobianco J, Vetrone F, Boyer J, Speghini A, Bettinelli M. Enhancement of Red Emission ($^4F_{9/2} \rightarrow ^4I_{15/2}$) *via* Upconversion in Bulk and Nanocrystalline Cubic Y_2O_3:Er^{3+} J Phys Chem B. 2002; 106:1181–1187.

58. Svanberg, S. Atomic and Molecular Spectroscopy: Basic Aspects and Practical Applications. Springer-Verlag; New York: 2004. p. 106-107.
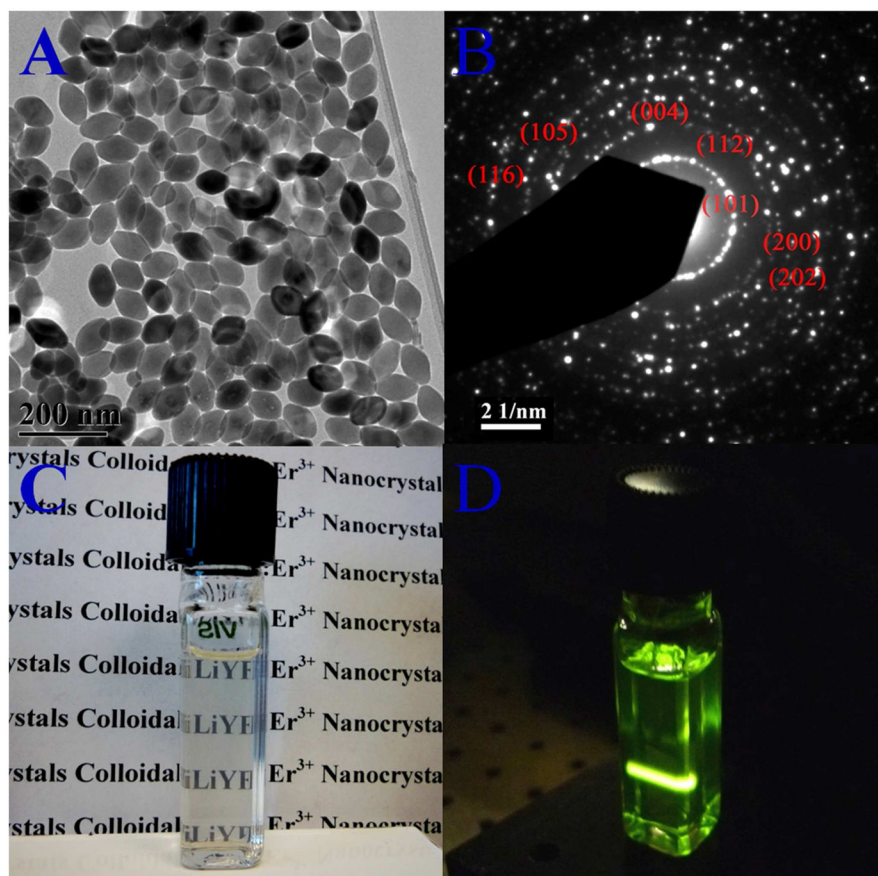
Figure 1.
(A) Transmission electron microscopy (TEM) image of $LiYF_4$:10% Er^{3+} nanocrystals. (B) Selected area electron diffraction pattern (SAED) of $LiYF_4$:10% Er^{3+} particles. (C) Photographic image of a colloidal suspension of $LiYF_4$:10% Er^{3+} nanocrystals in chloroform. (D) Photographic image of upconversion PL in 1 wt% colloidal $LiYF_4$:10% Er^{3+} nanocrystals under unfocused laser excitation at 1490 nm of 4 W/cm^2.
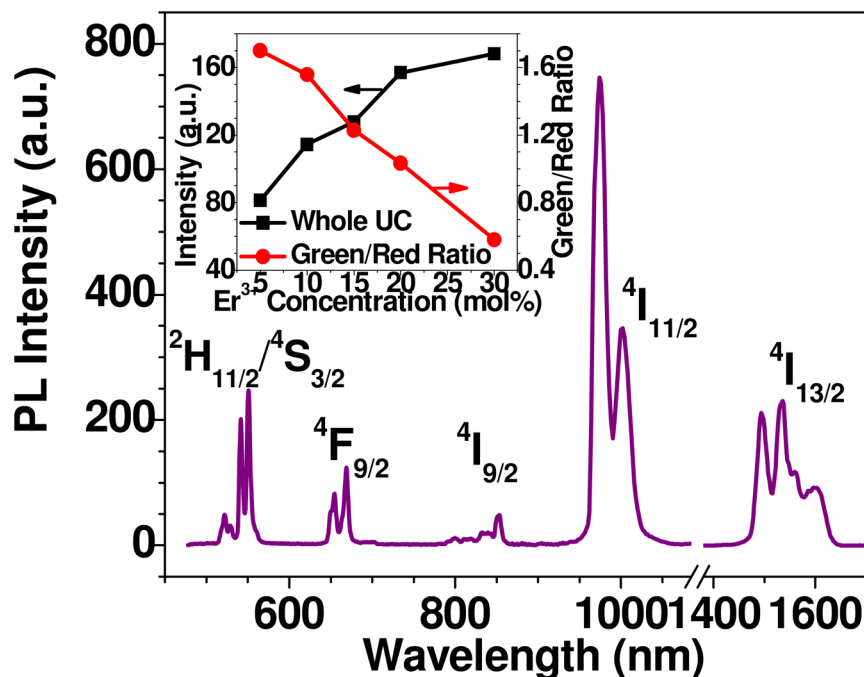
Figure 2.
Calibrated PL spectra of colloidal LiYF$_4$:10% Er^{3+} nanocrystals under laser excitation at 1490 nm (chloroform suspension). The scattering from the excitation laser was corrected using the PL spectrum of the Er^{3+} ions at ~1500 nm obtained under excitation with a 975 nm laser diode. The inset shows the dependences of upconversion PL intensity and the green/red ratio (ratio between intensities of the green emission at 550 nm and the red one at 670 nm) on the Er^{3+} concentration.
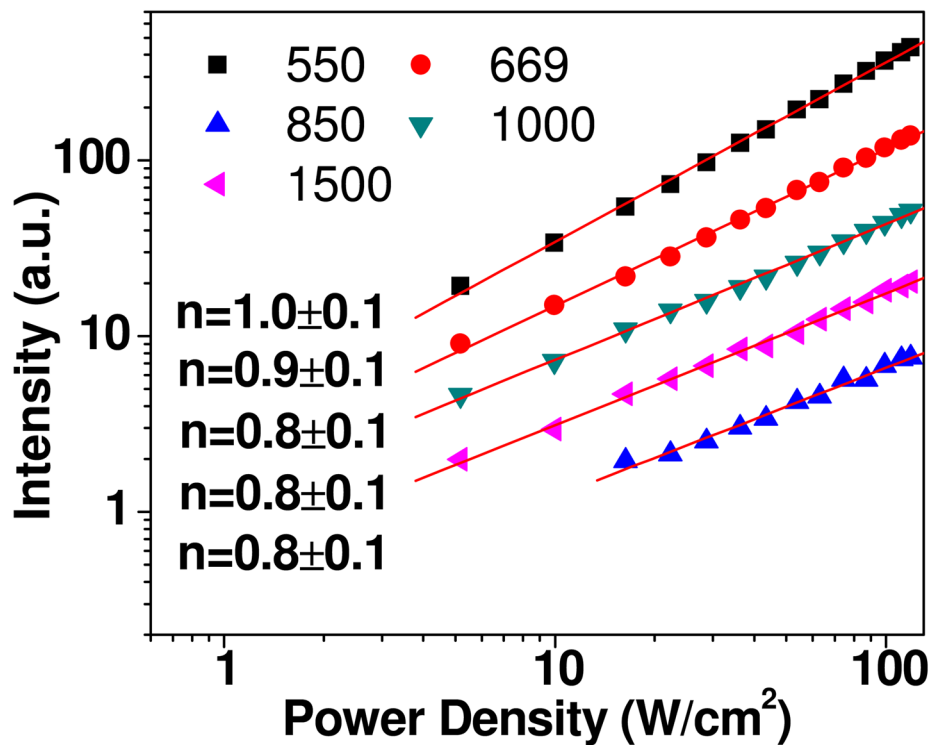
Figure 3.
The dependence of the intensities of all emissions bands on the power of excitation at 1490 nm in colloidal LiYF$_4$:10% Er^{3+} nanocrystals.
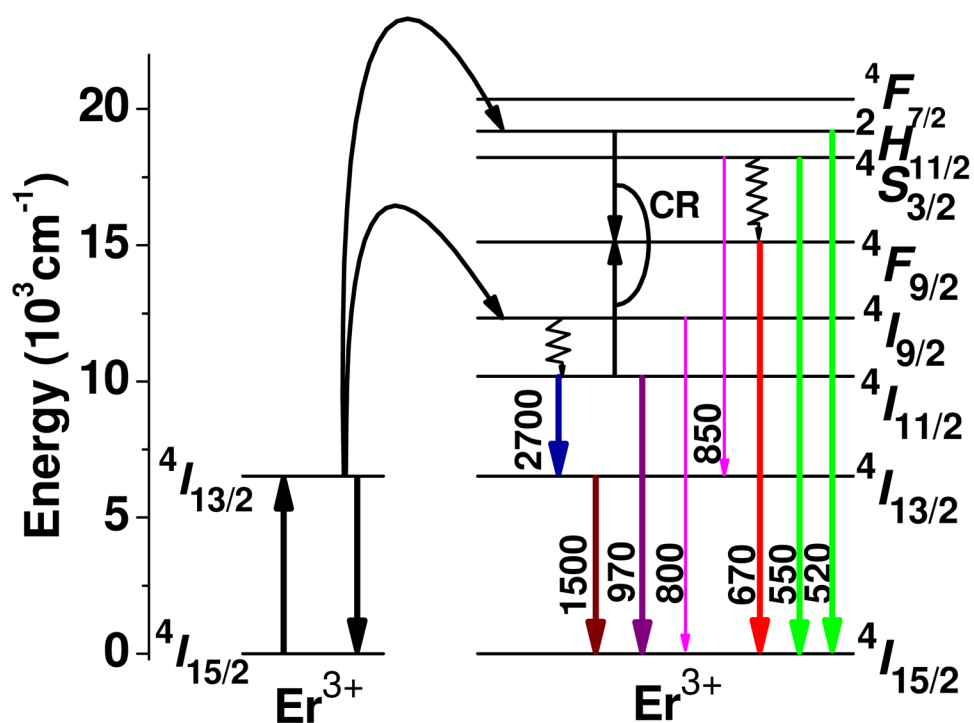
Figure 4.
Diagram of the energy levels of Er^{3+} ion and the proposed mechanisms of upconversion.